International Journal of Polymer Analysis and Characterization

ISSN: 1023-666X (Print) 1563-5341 (Online) Journal homepage: https://www.tandfonline.com/loi/gpac20

Corn oil based poly(urethane-ether-amide)/fumed silica nanocomposite coatings for anticorrosion application

Manawwer Alam

To cite this article: Manawwer Alam (2019) Corn oil based poly(urethane-ether-amide)/fumed silica nanocomposite coatings for anticorrosion application, International Journal of Polymer Analysis and Characterization, 24:6, 533-547, DOI: 10.1080/1023666X.2019.1622719

To link to this article: https://doi.org/10.1080/1023666X.2019.1622719

Published online: 07 Jun 2019.

INTERNATIONAL JOURNAL OF POLYMER ANALYSIS AND CHARACTERIZATION
2019, VOL. 24, NO. 6, 533–547
https://doi.org/10.1080/1023666X.2019.1622719

Taylor & Francis
Taylor & Francis Group

Corn oil based poly(urethane-ether-amide)/fumed silica nanocomposite coatings for anticorrosion application

Manawwer Alam

Department of Chemistry, College of Science, King Saud University, Riyadh, Saudi Arabia

ABSTRACT

Poly(urethane-ether-amide) (PUIEtA) nanocomposite coatings on mild steel were prepared by using corn oil, isosorbide and isophorone diisocynate and fumed silica. The syntheses steps were confirmed by FTIR, ^{1}H NMR and ^{13}C NMR spectroscopy techniques. The morphology of PUIEtA nanocomposite coating was studied by SEM-EDX, that confirmed the presence of nanosilica and thermal behavior was studied by DSC/TGA analysis. The anticorrosion performance of PUIEtA coating systems on mild steel, exposed to 3.5 wt% NaCl solution, was evaluated using electrochemical impedance spectroscopy. Scratch hardness, pencil hardness, adhesion, and bending test were performed in order to investigate the performance of nanocomposite coating on mild steel substrate. It was found that PUIEtA-fumed silica nanocomposite coating could provide much better protection than PUIEtA. PUIEtA-3 nanocomposite coating can be safely used up to 200 °C.

ARTICLE HISTORY
Received 4 April 2019
Accepted 18 May 2019

KEYWORDS
Corn oil; isosorbide; polyetheramide; urethane; corrosion

Introduction

The use of sustainable resources, in the development of corrosion protection coatings, as an alternative source to petro-based chemicals has gained significant importance. Inexpensive vegetable oils have been used for the fabrication of valuable polymeric resins.[1] Lately, substantial research has been focused on the production of bio-based polymeric resins using vegetable oils. Vegetable oils based epoxies, polyurethanes, polyesteramides, polyetheramides, alkyds and composites have been developed from oils of linseed, corn, jatropha, soyabean, castor, pongamia, rapeseed, coconut and others.[2–4]

Polyurethane (PU) elastomers find important application as barrier materials for transport ions. The behavior of polyurethane is controlled by polymer structure and crosslink density. PU coatings exhibit excellent abrasion resistance, toughness, low temperature flexibility, corrosion resistance, chemical resistance, mechanical strength and low toxicity. Due to these characteristics, PU coatings have emerged as coatings of choice for application on mild steel.[5,6] Various isocyanates like toluene diisocyanate (TDI), methylene bis(cyclohexylisocyanate), isophorone-diisocyanate(3-isocyanatomethyl-3,5,5-trimethylcyclohexyl isocyanate) (IPDI) are used for the preparation of polyurethane. IPDI was found less reactive than TDI, thus enhancing the pot life and minimizing defects of the synthesized PU.[7]

Isosorbide (1,4:3,6-dianhydro-D-sorbitol) is a bio-based plasticizer, a renewable monomer derived from glucose.[7] Isosorbide is a nontoxic, biodegradable, and thermally stable heterocyclic

CONTACT Manawwer Alam maalam@ksu.edu.sa Department of Chemistry, College of Science, King Saud University, P.O. Box 2455, Riyadh 11451, Saudi Arabia.
Color versions of one or more of the figures in the article can be found online at www.tandfonline.com/gpac.

diol and its structure is very suitable for polycondensation or polyaddition reactions,[8] which makes it useful in biomedical applications. Isosorbide is increasingly used in polymer synthesis with characteristics such as rigid structure and low toxicity and is also used in the synthesis of linear polyurethanes with different soft segments and aliphatic or aromatic diisocyanates, attractive for different applications.[8] Isosorbideis used in the synthesis of diesters,[7] polyesters,[8–10] polyacetals,[11] polycarbonates[12,13] water-borne polyurethanes[8] and isocyanate-free polyurethanes.[14] Isosorbide and their derivatives are also used for optically active polyamides,[15] optically active polyurethanes[14] and cross-linked polyurethanes.[8,15] These polymers biodegradable and biocompatible and are also used for UV curable coatings.[16] UV-cured organic coatings should combine specific properties, such as adhesion to substrates, low friction, resistance to environmental stresses, and other interesting properties.[8,17,18]

To improve the properties of organic coating many metal oxides used such as ZnO, TiO_2, SiO_2 and carbon fillers.[19–22] Fumed silica has high super hydrophobicity and highly flexible properties. Fumed silica enhances the mechanical properties of coatings and improves its barrier property in corrosive media. So fumed silica containing coatings have superior anticorrosive performance due to silica in polymer matrix.[23,24]

The main objective of this study is to develop a new type of green nanocomposite material consisting of corn oil and isosorbide, both sustainable resource based materials. In this work, we developed new coating materials with improved, useful properties, by using isosorbide. The developed PUIEtA-FS nanocomposite was characterized by various techniques such as FTIR, ^{1}H NMR, ^{13}C NMR and SEM-EDX. Thermal stability and curing behavior was studied by thermogravimetric analysis (TGA)/DTG and DSC. Electrochemical impedance spectroscopy (EIS) technique was used to evaluate the corrosion resistance performance of PUIEtA-FS nanocomposite in saline environment.

Experimental

Materials and methods

Corn oil (Afia International Company, Jeddah, Saudi Arabia),[3,25] Isosorbide (Alfa Asear, UK), sodium metal, methanol, toluene (BDH Chemicals, Ltd., Poole, England), fumed silica (0.2–0.3 μm average particle size, $200 \pm 25\ m^2\ g^{-1}$ surface area, Sigma Aldrich, USA), dibutyltindilaurate (DBTDL), and isophorone diisocynate (Acros Organic, USA) were used as received.

FTIR, ^{1}H NMR and ^{13}C NMR were used to elucidate the chemical structure of synthesized materials. FTIR spectra of these resins were taken on KBr cell on Spectrum 100 (Perkin Elmer Instrument, USA). ^{1}H NMR and ^{13}C NMR were recorded on JeolDPX400MHz spectrometer (Japan) using deuterated dimethyl sulfoxide as solvent and tetramethylsilane as internal standard. Thermal stability and curing behavior of nanocomposite was studied by TGA/DSC (Mettler Toledo AG, Analytical CH-8603, Schwerzenbach, Switzerland) at constant heating rate $10\ ^\circ C\ min^{-1}$ in nitrogen atmosphere. The morphology and composition were investigated on FE-SEM and EDX (JEOL JSM7600F, Japan). Thickness, scratch hardness, cross-hatch adhesion, conical mandrel bending, pencil hardness and gloss tests were performed according to a previously reported work.[26] The working electrode-coated metal specimens were covered by a fixed PortHoles electrochemical sample mask with an exposed surface area of $1.0\ cm^2$ in 3.5 wt% NaCl corrosive media. EIS study was performed by an Autolab potentiostat/galvanostat, PGSTAT204-FRA32, with the NOVA 2.0 software (MetrohomAutolab B.V. Kanaalweg 29-G, 3526 KM, Utrecht, The Netherlands) using a three-electrode system such as counter (platinum), reference (Ag/AgCl) at room temperature. EIS spectra were obtained in frequency range of 100 Hz–1 MHz with amplitude of 10 mV with 10 points per decade and electrolyte used was 3.5 wt% NaCl solution.

Synthesis of N,N-bis(2-hydroxy ethyl) corn oil fatty amide (HECA)

HECA was synthesized according to previously published work.[3,25]

Synthesis of poly(isosorbide-ethermide) (PIEtA)

PIEtA was synthesized by reacting HECA (1.0 mol) and Isosorbide (1.0 mol) with one drop of dilute (1:1) sulfuric acid as catalyst, in a four neck round bottom flask with thermometer, mechanical stirrer, nitrogen inlet and dean stark trap. The mixture was initially heated at 90 °C for completion of reaction and monitored by thin layer chromatography (TLC). After completion of reaction, toluene was added for azeotropic distillation and temperature was increased up to 120 °C until theoretical amount of water was collected in dean stark trap. At the end of reaction, PIEtA was taken out from round bottom flask and toluene was withdrawn from PIEtA using rotary evaporator under reduced pressure.

Synthesis of poly(isosorbide urethane etheramide) (PUIEtA) and PUIEtA/FS nanocomposite

PIEtA (5.00 g) was dissolved in toluene and calculated amount of IPDI (40 wt%, previously selected after optimization, based on drying performance of coatings) with 0.5 wt% DBTDL catalyst based on resin was added. The contents were heated at 120 °C, and for 30 min, under continuous stirring to obtain PUIEtA. To this prepared PUIEtA resin was added 1, 2, 3 wt% fumed silica (solution made in toluene and kept on ultrasonic bath for 15 min at room temperature), under continuous stirring at 120 °C for 30 min, and these resins were denoted as PUIEtA-1, PUIEtA-2, PUIEtA-3, the numbers representing the percent loading of FS. The progress of the reaction was monitored by TLC.

Results and discussion

The reaction in Schemes 1 and 2 depicts the synthesis of PIEtA and PUIEtA. Synthesis of PIEtA was accomplished by the combination of HECA and isosorbide. The free OH groups of PIEtA were treated with IPDI to obtained PUIEtA and further FS was added in different percentage to obtain a series of nanocomposite resins. The structural elucidation of PIEtA and PUIEtA was ascertained by using FTIR, ^{1}H NMR and ^{13}C NMR. The hydroxyl value (OH group per 100 g) (14.214, 4.280, 3.901, 3.134, 2.764) decreased from PIEtA to PUIEtA-3, in descending order: PIEtA > PUIEtA > PUIEtA-1 > PUIEtA-2 > PUIEtA-3. PUIEtA-3 resin is soluble in pentane 2-one, ethyl methyl ketone, choloroform, methanol, ethanol, ethyl acetate, n-hexane, dimethyl formamide (DMF), dimethylsulfoxide (DMSO), toluene, xylene, acetone, benzene, pyridine, carbon tetrachloride, tetrahydrofuron, foramamide and partially soluble in diethyl ether. 40% solution of PUIEtA used for preparation of coating on mild steel.

Spectral analysis

Figure 1 shows FTIR spectra of PIEtA and PUIEtA-2. PIEtA spectrum has characteristic band of ether linkages at 1212.13 cm^{-1} (C – O–C, asymmetrical stretching vibration).[3] Other related bands such as 3368.46 (OH), 3010.11 (–C = C–), 2925.85 (CH_2 str. asymmetrical), 2854.86 (CH_2 str. Symmetrical.), 1620.80 (CO, amide), 1465.93 (C – N, str), 1079.16 (C – O–C, asymmetrical stretching vibration, C – O in C – OH), 1009.31, 977.75, 884.62, 834.69, 794.71, 722.36 (CH, bending) are also observed. In case of **PUIEtA-2,** 3334.77 (NH, urethane), 2259.16 (NCO), 1704.44 (CO, urethane), 1626.22, 1547.89, 1464.75, 1245.00 (C-O-C stretching vibration), 1048.75, 865.09, 804, 704.85, 608.31 (str., and bending. O – Si – O) are observed in FT IR spectrum.

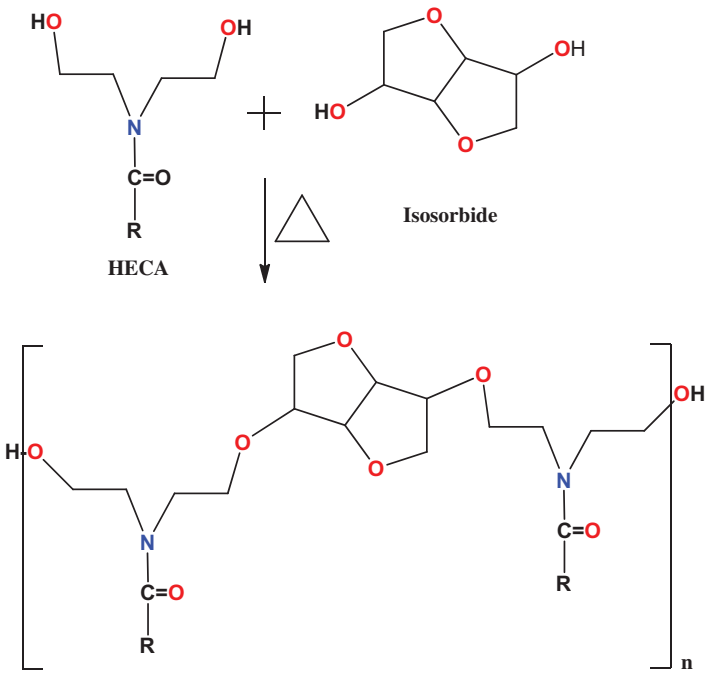

Scheme 1. Synthesis of PIEtA.

PIEtA; ^{1}H NMR(DMSO-d_6) δ ppm: 0.840(−C**H**$_3$); 1.217(−C**H**$_2$−); 1.447(−C**H**$_2$−CH$_2$−CO); 1.955(−CH = CH − C**H**$_2$−); 2.282(−C**H**$_2$−CO); 2.716(=CH − C**H**$_2$−CH=); 3.232 and 3.70(−C**H**$_2$ −N); 3.301 to 3.688(C**H** and C**H**$_2$ of heterocyclic ring of Isosorbide); 4.015(−C**H**$_2$−OH); 4.217(−CH$_2$−O−); 4.852(CH$_2$−O**H**); 5.323(−C**H**=C**H**−) of PIEtA (Figure 2). In case of PUEItA some additional peaks like 7.964(−N**H**, urethane); 4.233(C**H**$_2$−CONH) are shown in Figure 3.

PIEtA; ^{13}C NMR(DMSO-d_6) δ ppm: 13.969(−**C**H$_3$); 22.021(−**C**H$_2$−CH$_3$); 25.521(**C**H$_2$−CO); 27.154(−**C**H$_2$−CH = CH−); 28.671 to 29.135 (chain −**C**H$_2$−); 31.143 to 32,742(−**C**H$_2$−CH$_2$ −CO); 48.338(−**C**H$_2$−N<, near OH); 50.566(−**C**H$_2$−N<, near − O−); 58.913(−**C**H$_2$−OH); 59.188(–**C**H$_2$–O–); 70.841 to 72.308(–CH$_2$–, isosorbide); 75.290(>**C**H–, isosorbide); 81.291, 87.754(–O–**C**H–O); 127.770 to 129.745(–**C**H=**C**H–); 172.498(–**C** = O–, amide) (Figure 4), In **PUEItA** some additional peaks 161.501(–**C**ONH); 151.213(free, N**C**O); 63.083(–CH$_2$–**C**H$_2$ –CONH); –**C**H$_3$ and cyclic ring carbon of IPDI peaks are same region as PIEtA are shown in Figure 5.

FE-SEM and EDX analysis

The morphology of PUIEtA-1 and PUIEtA-2 on the coating surfaces was investigated using FE-SEM (Figure 6(a,b)). It can be seen that all fabricated coatings show uniform and homogeneous, close-packed structure and adherent film on mild steel, leading to good corrosion resistance of mild steel with PUIEtA coatings incorporated with fumed silica. This confirms that the coating layer is completely covering the surface of mild steel panel. In EDX analysis, the weight percentages of Si found on the surface of PUIEtA-1 and PUIEtA-2 coatings were 0.90 and 1.78%. FE-SEM image shown in Figure 6(a,b) also confirm that Si nanoparticles are homogeneously distributed over the entire surface of the coating.

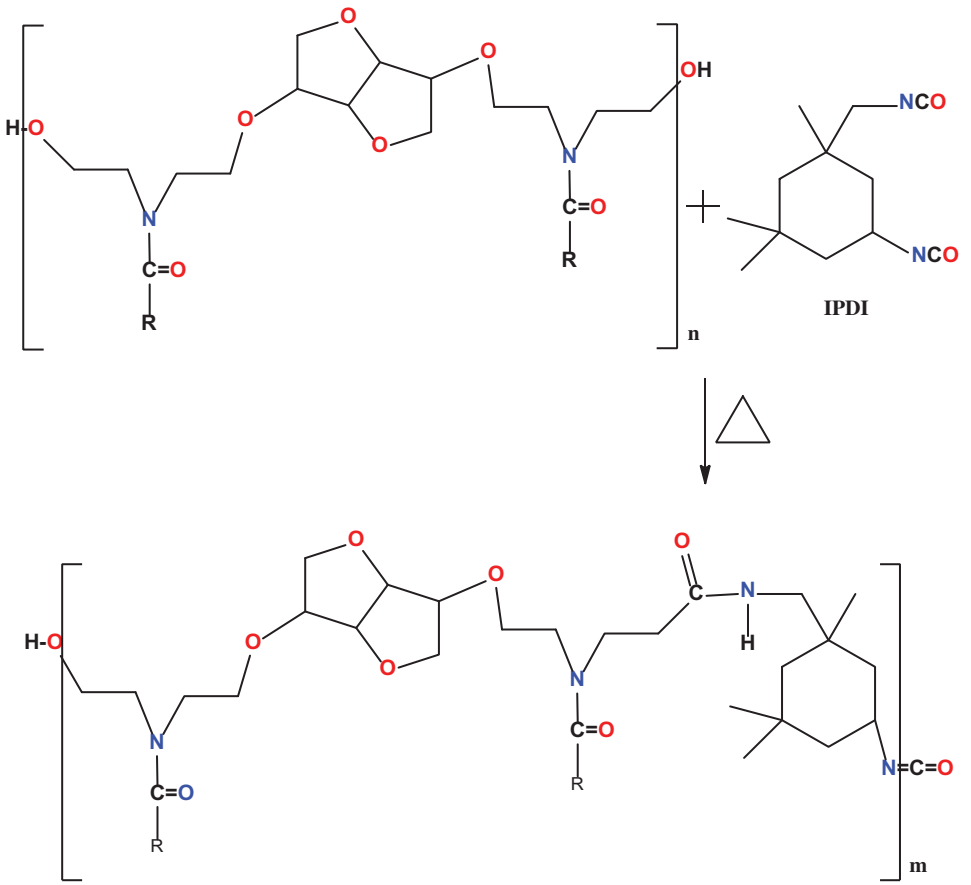

Scheme 2. Synthesis of PUIEtA.

Physico-mechanical properties

PUIEtA coatings are made by drying at room temperature. The coating thickness was found to be $150 \pm 5\,\mu$m. The scratch hardness values of PUIEtA coatings increased from PUIEtA (1.5 kg) to PUIEtA-1 (2.4 kg), PUIEtA-2 (2.8 kg) and PUIEtA-3 (2.5 kg), beyond which the scratch hardness value deteriorated. The pencil hardness values were obtained to be 1B (PUIEtA), 3H (PUIEtA-1), 4H (PUIEtA-2), and 1H (PUIEtA-3), deteriorating beyond PUIEtA-2, i.e., beyond 2 wt% loading of fumed silica in PUIEtA resin. The coatings showed good impact resistance (150 lb inch^{-1}), bending ability (1/8 inch) and the cross-hatch test results were 98%. The Gloss values at 45° were found 72(PUIEtA), 81(PUIEtA-1), 83(PUIEtA-2), and 87(PUIEtA-3). Beyond 3 wt% loading, the performance of the coatings deteriorated. Silica particles increase the adhesion, flexibility and impact resistance of coatings due to good interaction between organic and inorganic phases. Beyond 3 wt% loading, there may be insufficient interaction between organic moieties and inorganic silica phases, due to overloading of silica. The fumed silica particles occur as aggregates, allowing for particle-particle interactions and compactness in aggregates, with more silica inclusion, the compactness between particles increases so much that it leads to rigidity, stiffness and brittleness in PUIEtA coatings.[26,27]

Corrosion studies

The EIS techniques is based on AC impedance over a period of immersion time to estimate the barrier effect of PUIEtA-2 coating on mild steel. The change of parameters in a simulated

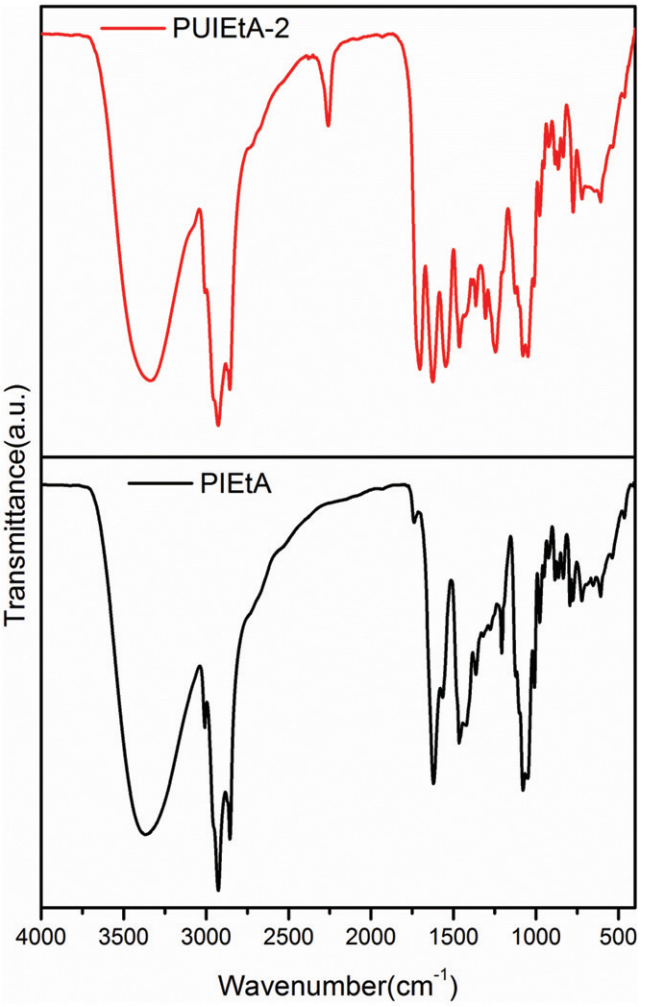

Figure 1. FT IR spectra of PIEtA and PUIEtA-2.

equivalent circuit (Figure 7) is used to indicate the change of structure and corrosion resistance of PUIEtA-2 coatings. The value of parameter related with the high frequency part has shown coating capacitance (C_{coat}) and lower frequency part has shown coating resistance (R_{coat}), which are considered to be PUIEtA-2 coating properties changed with immersion time. Coating capacitance and coating resistance have the following relation:

$$Ccoat = \frac{1}{2\pi f Rcoat}$$

where f is the frequency. In equivalent circuit (Figure 7) coating resistance is inversely proportional to coating capacitance. Solution resistance (Rs), coating capacitance (Cc). It is sometimes used to monitor water adsorption in coating because dielectric constant of electrolyte is greater than polymers, Charge transfer resistance (Rct) and film resistance (resistance to charge transport through pores, voids, and other defects in coating), Cdl (double layer capacitance, that arises from dipole interactions on metal surface) and constant phase element (CPE).

Nyquist plots of PUIEtA-2 coatings are obtainedfor different immersion times (4, 8, 12, 16, 20, and 24 days) in 3.5 wt% NaCl solution (Figure 8). Nyquist plots of PUIEtA-2 in all immersion

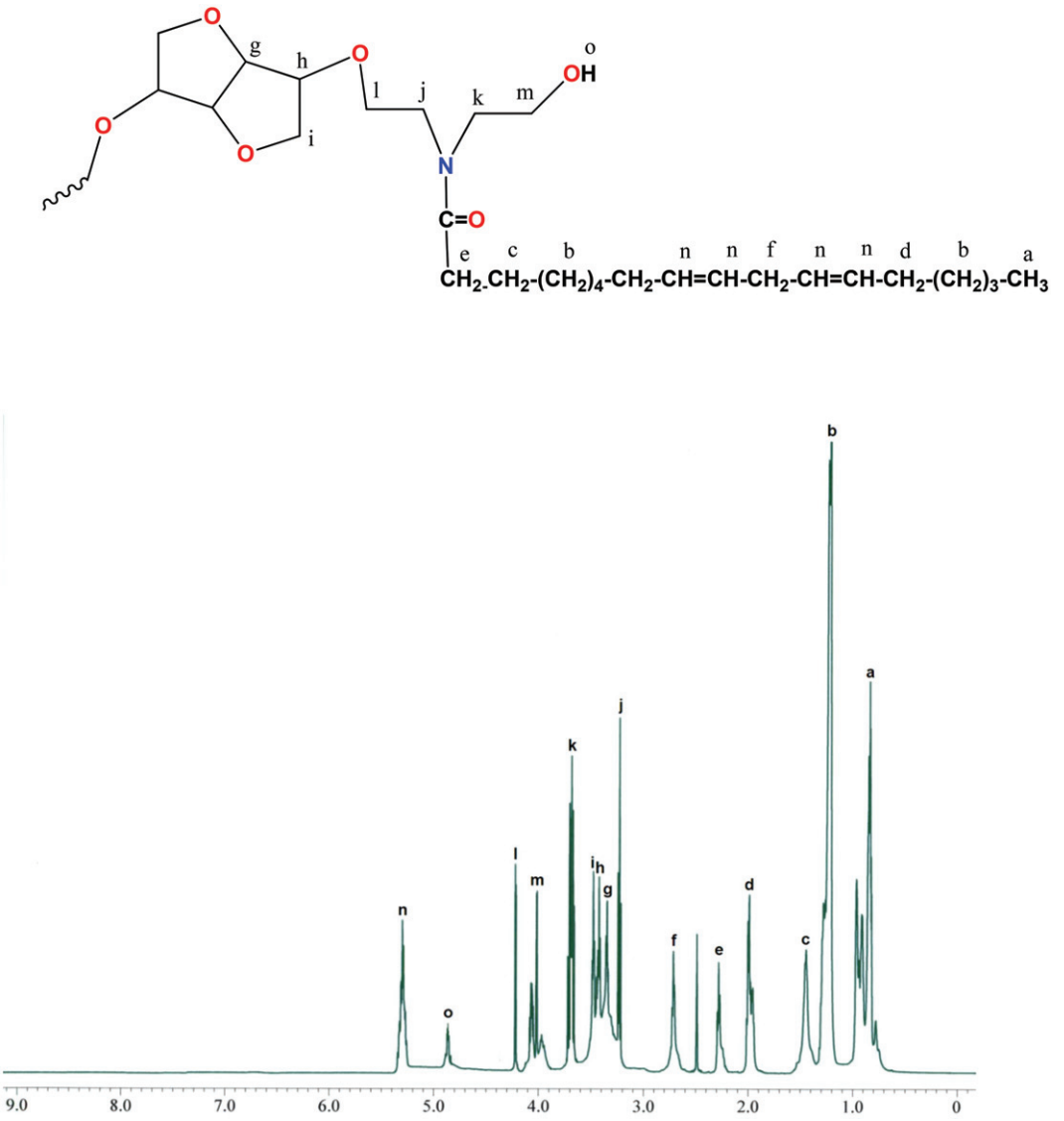

Figure 2. ^{1}H NMR spectra of PIEtA.

times have shown only one type of equivalent circuit model (Figure 7). After 4 days of immersion time, PUIEtA-2 coating reveals that it is dominated by coating capacitance at high frequency and coating resistance at low frequency. The perfect coatings often exhibit an excellent barrier performance resulting in a large impedance of metal/PUIEtA-2 coating due to nano SiO_2 in organic PUIEtA coatings. One semicircle indicates that charge transfer process of PUIEtA coating on mild steel is shown as rate determining step of corrosion process. However, deviation from perfect semicircle indicates some inhomogeneity or roughness of mild steel surface. With increases of immersion time up to 24 days accumulation of corrosive ions occurs at metal/coating interface. The immersion time increases and semicircle diameter decreases as shown in Nyquist plot, which denotes the break-down of coating due to delamination and corrosion accumulation. The circuit simulated results of charge transfer resistance as function of immersion time for the PUIEtA-2. The coating resistance decreased with increases immersion time (Table 1).

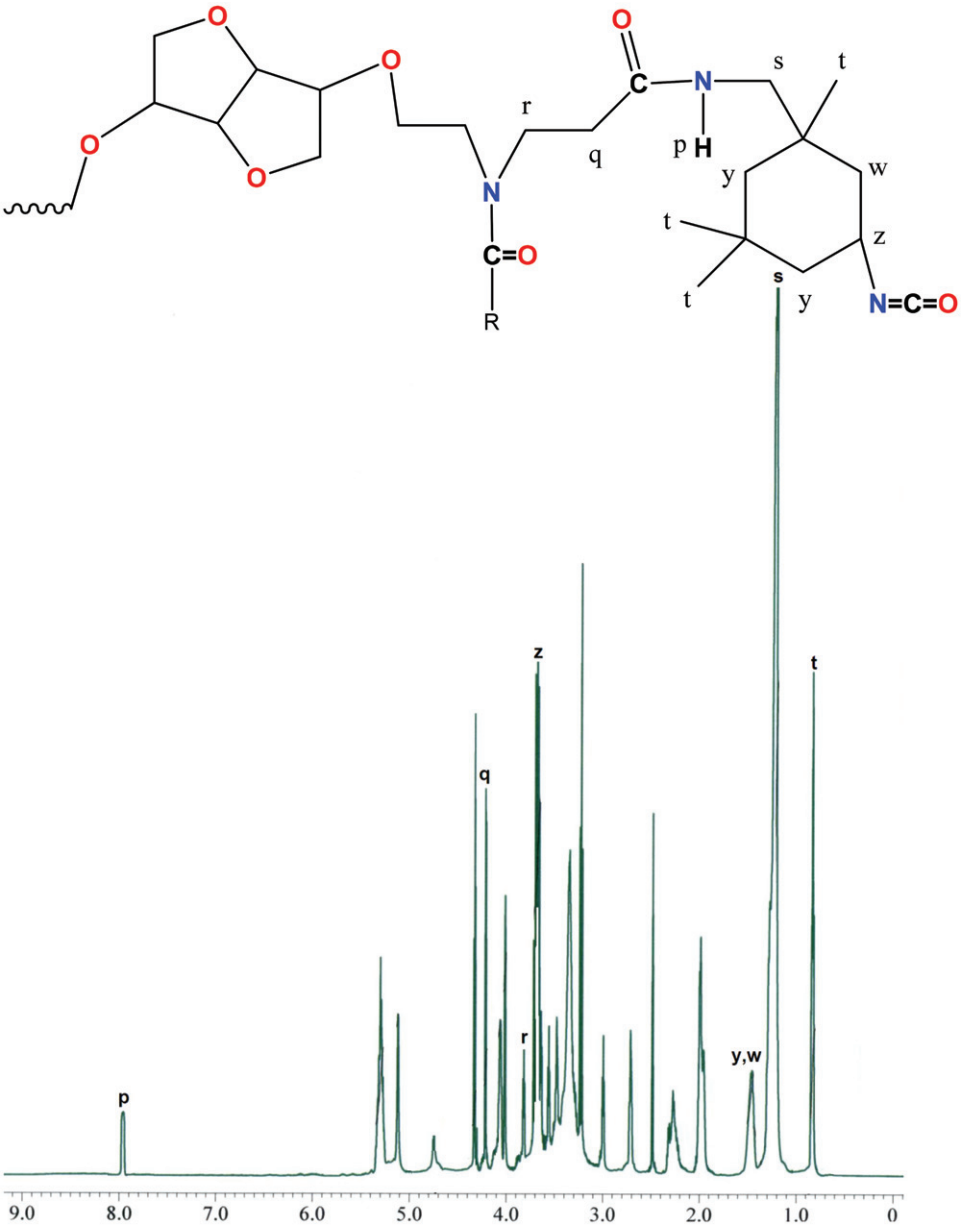

Figure 3. ^{1}H NMR spectra of PUIEtA.

Figure 9 shows the bode diagram of PUIEtA-2 at different immersion times in 3.5 wt% NaCl solution. With increasing immersion time, the modulus in low frequency range decreased gradually. The phase angle plot shows that with increased immersion time, frequency is decreased. In any immersion time, high frequency region is related to capacitance and low frequency region to resistance of PUIEtA-2 coating. In the other words, low frequency is related with the reaction resistance and double layer capacitance. After 24 days immersion time, the modulus decreased from 6.6×10^5 to 1.0×10^5 Ω, which belongs to delamination of coatings.[28–30] The solution was saturated after 24 days and micro-cells were formed on PUIEtA-2 coating interface.

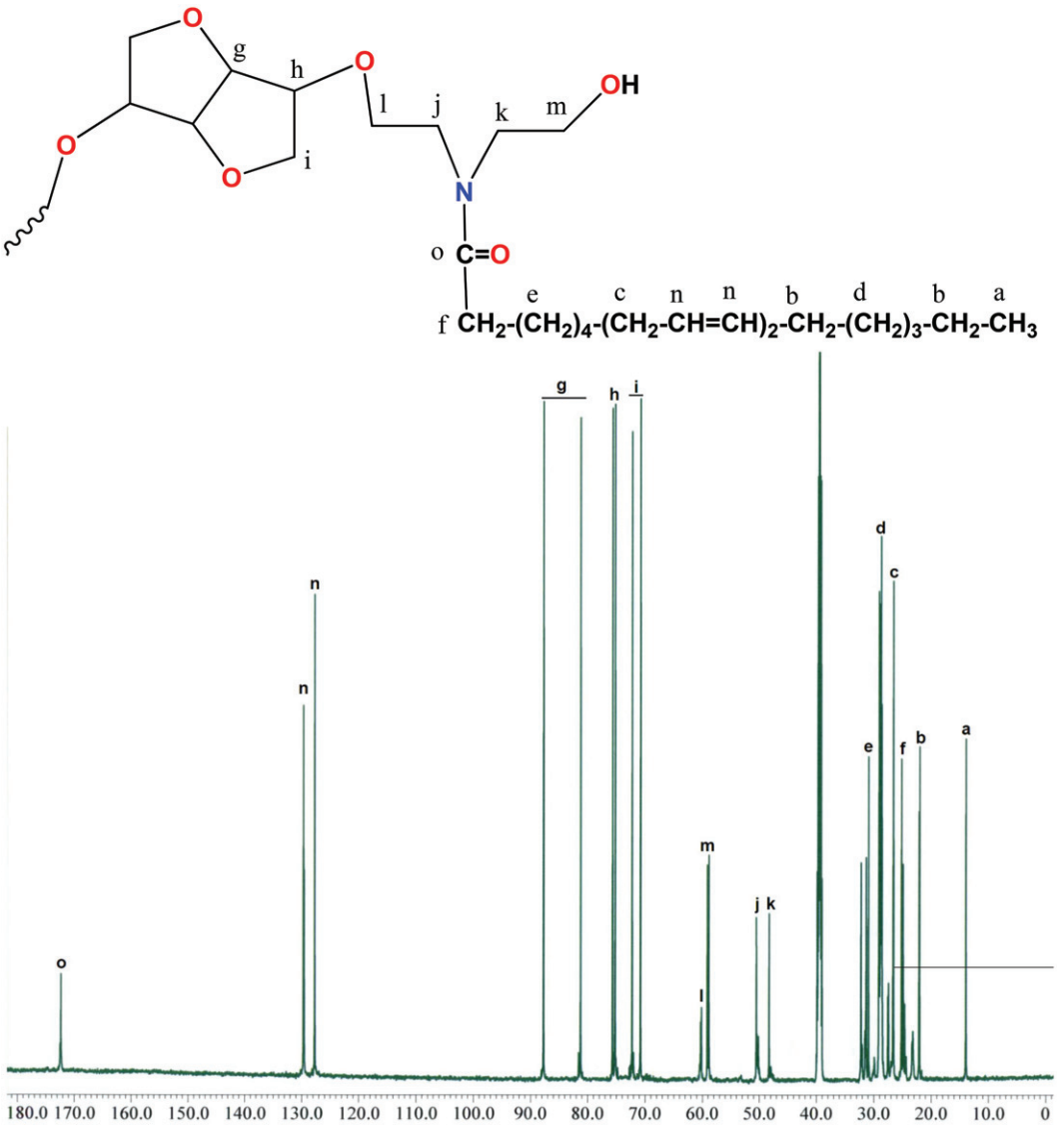

Figure 4. ^{13}C NMR spectra of PIEtA.

Thermal analysis

Figure 10 represents the TGA curve of PIEtA, PUIEtA and fumed silica modified PUIEtA (1,2,3), respectively. PUIEtA-coated materials show two-step decomposition, confirmed by DTG (Figure 11). 5% weight loss of each sample at 265.67, 256.18, 259.97, 261.87 and 275.16 °C respectively, corresponds to the loss of solvent. 50% weight loss occurs at 403.82, 367.75, 388.64, 419.01, and 401.93 °C due to thermal decomposition. DTG thermograms of PIEtA, PUIEtA and fumed silica modified PUIEtA-1, PUIEtA-2, and PUIEtA-3 coating clearly show every decomposition (Figure 11). First decomposition peak of PIEtA starts from 200.54 to 383.52 °C centered at 328.03 °C and second up to 560.82 °C and centered at 438.87 °C. This range belongs to 50% weight loss in TGA thermogram. In case of PUIEtA and fumed silica modified PUIEtA-1, PUIEtA-2, and PUIEtA-3 coatings, first decomposition starts from 200.68, 201.41, 210.90, 212.80 to 393.46, 394.33, 392.43, 396.23, 394.33 °C centered at 320.14, 331.97, 321.02, 325.11, 323.06 °C

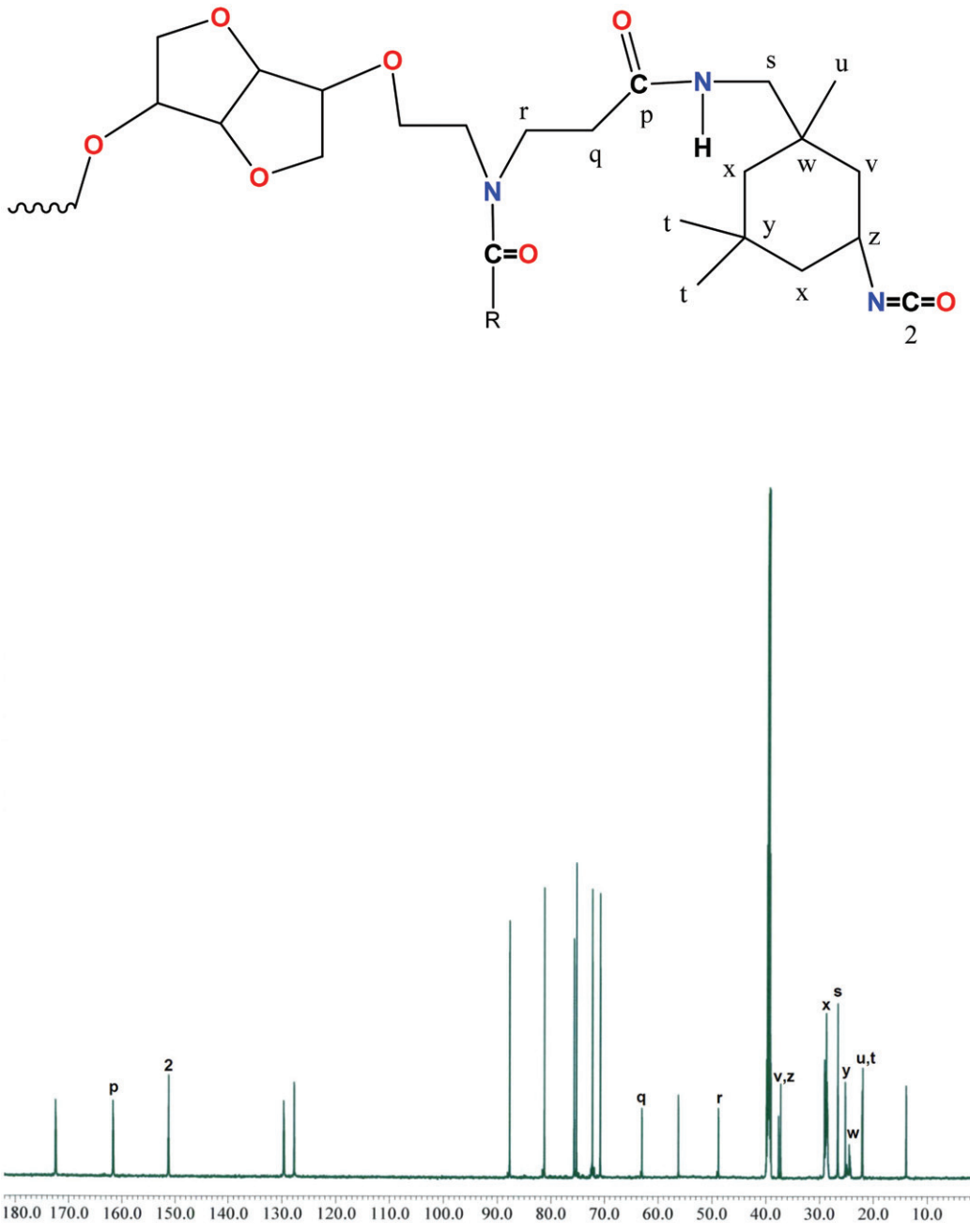

Figure 5. ^{13}C NMR spectra of PUIEtA.

and up to 554.83, 554.68, 551.68, 550.74, 552.64 °C and centered at 487.51, 476.70,485.61, 487.51, 42.54 °C. The decomposition trend is similar in all materials. First and second decomposition peaks belong to urethane, ether, amide linkage and hydrocarbon chains, respectively. After the addition of fumed silica in PUIEtA coatings, slightly shifting the peaks of PUIEtA-1, PUIEtA-2, and PUIEtA-3 due to the strong attraction between silica nanoparticle and polymer matrix.

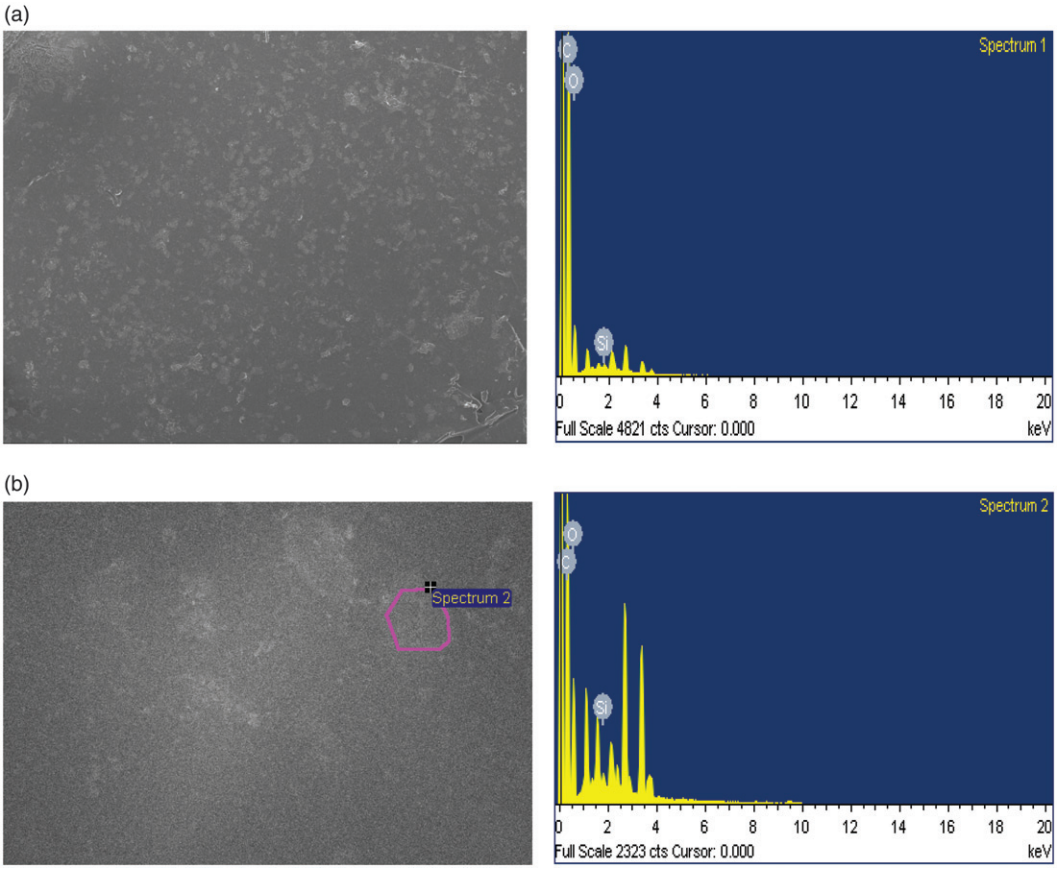

Figure 6. (a) FE-SEM/EDX of PIEtA-1 coatings; (b) FE-SEM/EDX of PIEtA-2 coatings.

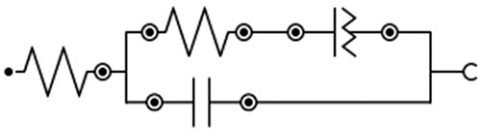

Figure 7. Equivalent circuit to fit the experimental data of PUIEtA-2.

Table 1. EIS data of PUIEtA-2 acquired by simulation in 3.5% NaCl solution.

Immersion time (days)	Rct (kΩ)	Rs (Ω)	Cdl (ρF)	CPE	
				Y_0 (μmho-s^n)	(n)
4	67.7	−625	175	2.78	0.981
8	75.6	−600	173	3.72	0.985
12	262	−525	169	11.8	0.988
16	357	1780	166	24.5	0.992
20	407	2170	158	30.5	0.997
24	456	2234	153	34.8	0.995

Conclusion

This study has presented a new polymer for the coatings of mild steel with global trend of using corn oil as natural resource rather than petroleum resources. These coating materials utilize isosorbide, which is also obtained from natural resource, inserting it into backbone of polymer chain

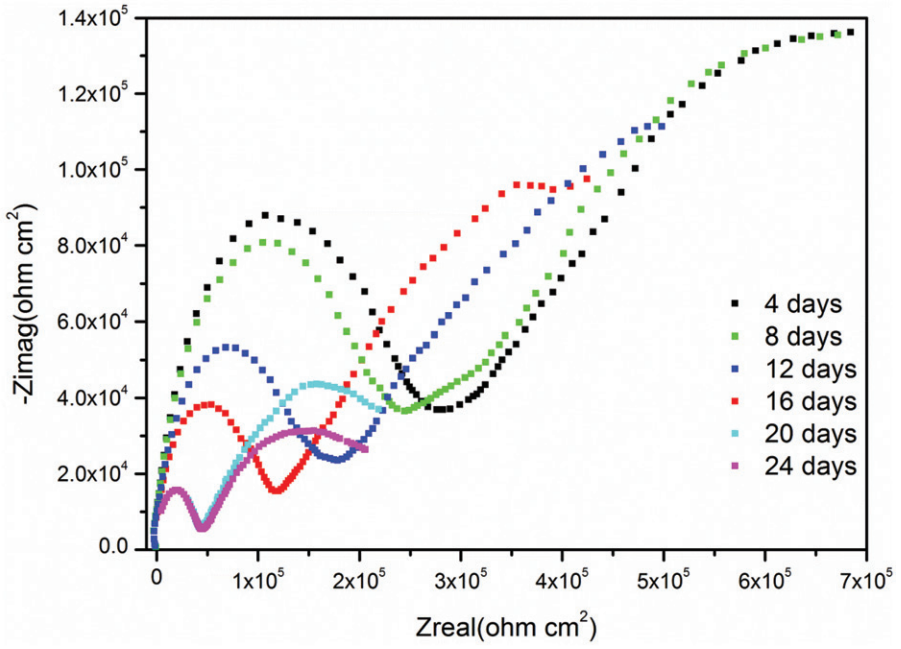

Figure 8. Nyquist plots of PUIEtA-2.

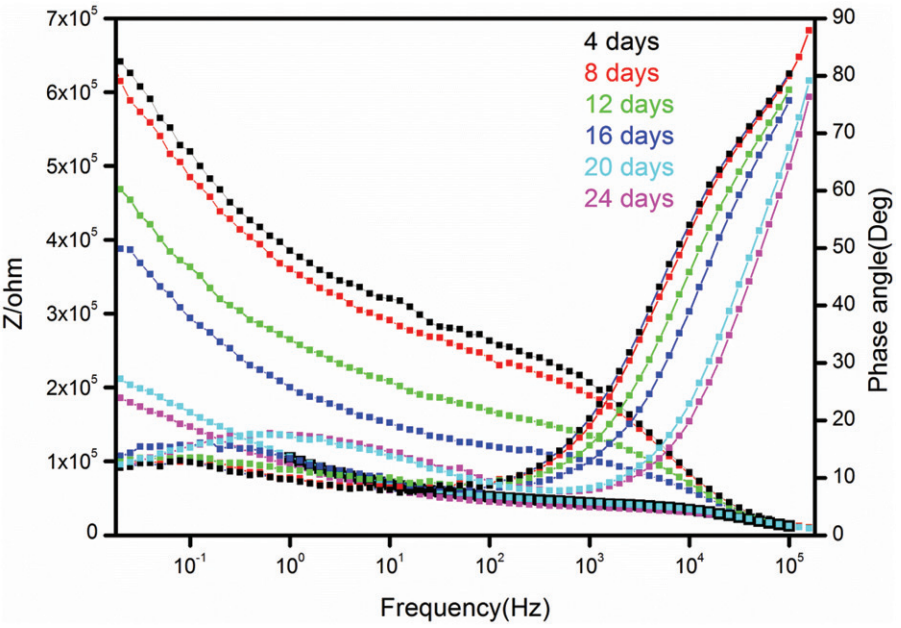

Figure 9. Bode plots of PUIEtA-2.

through a chemical reaction. These coatings are also environmentally friendly. Fumed silica has led to enhancement of mechanical and corrosion properties. The reaction between HECA and isosorbide, and further with IPDI has been confirmed by NMR and FTIR measurements. Additionally, it was concluded that the addition of silica has improved coating properties and thermal stability of coating materials.

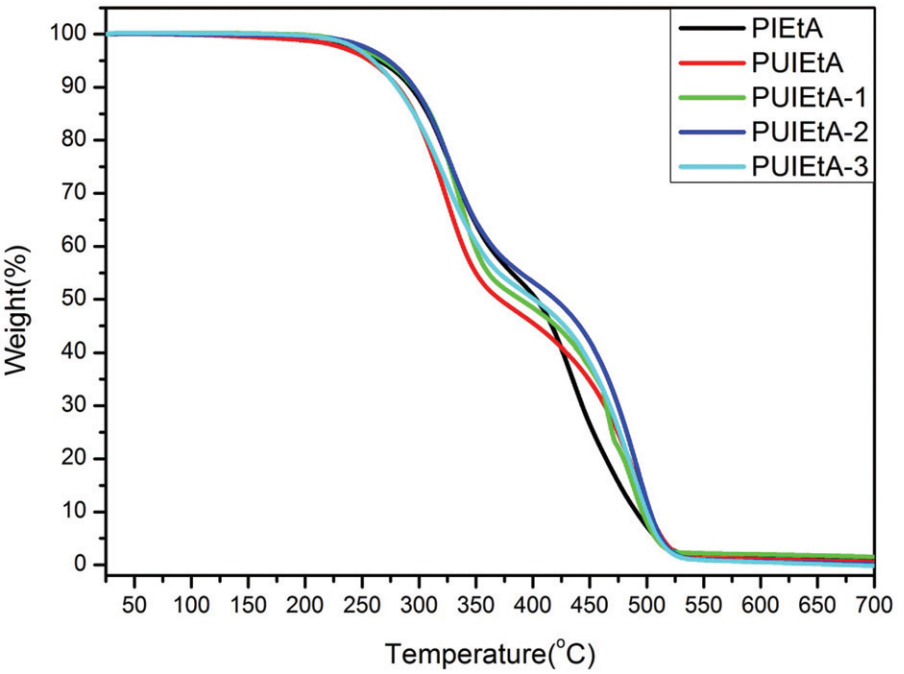

Figure 10. TGA thermogram of PIEtA, PUIEtA, PUIEtA-1, PUIEtA-2 and PUIEtA-3.

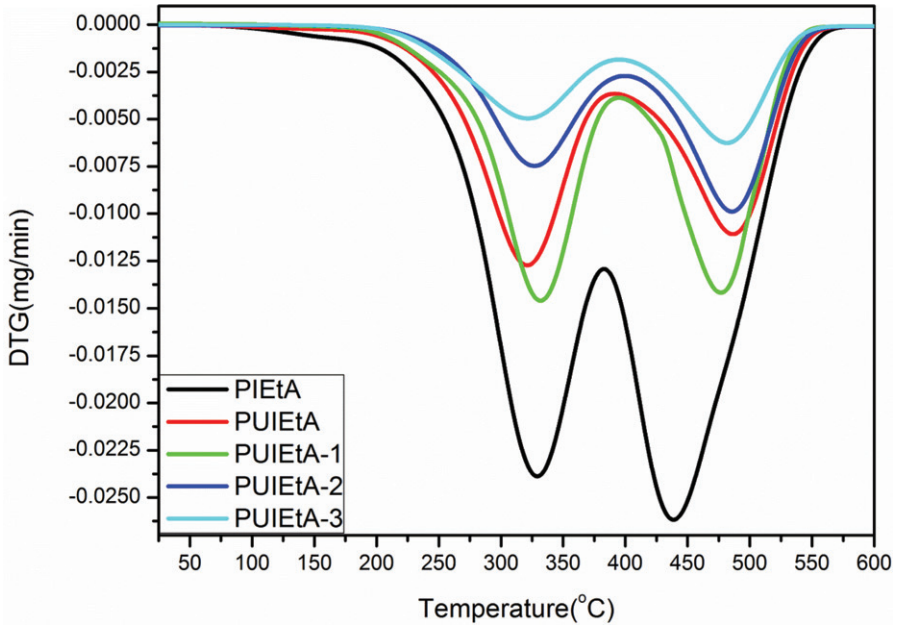

Figure 11. DTG thermogram of PIEtA, PUIEtA, PUIEtA-1, PUIEtA-2 and PUIEtA-3.

Funding

The Project was supported by King Saud University, Deanship of Scientific Research, College of Science – Research Center.

References

[1] Tsujimoto, T., H. Uyama, and S. Kobayashi. 2003. Green nanocomposites from renewable resources: biodegradable plant oil-silica hybrid coatings. *Macromol. Rapid Commun.* 24:711–714.
[2] Alam, M., D. Akram, E. Sharmin, F. Zafar, and S. Ahmad. 2014. Vegetable oil based eco-friendly coating materials: a review article. *Arab. J. Chem.* 7:469–479.
[3] Alam, M., and N. M. Alandis. 2014. Corn oil based poly(ether amide urethane) coatingmaterial—synthesis, characterization and coating properties. *Ind. Crops Prod.* 57:17–28.
[4] Sharmin, E., F. Zafar, D. Akram, M. Alam, and S. Ahmad. 2015. Recent advances in vegetable oils based environment friendly coatings: a review. *Ind. Crops Prod.* 76:215–229.
[5] Xu, Y., Z. Petrovic, S. Das, and G. L. Wilkes. 2008. Morphology and properties of thermoplastic polyurethane with dangling chain in ricinoleate-based soft segment. *Polymer* 49:4248–4258.
[6] Mannari, V. M., and J. L. Massingill. 2006. Two-component high-solid polyurethane coating system based on soy polyols. *J. Coat. Technol. Res.* 3:51–157.
[7] Ducrut, N., L. Delmotte, G. Schrodj, F. Stankiewicz, N. Desgardin, M.-F. Vallat, and B. Haidar. 2013. Evaluation of hydroxyl terminated polybutadiene-isophoronediisocyanate gel formation during crosslinking process. *J. Appl. Polym. Sci.* 128:436–443.
[8] Oprea, S., V.-O. Potolinca, and V. Oprea. 2016. Synthesis and properties of new crosslinked polyurethane elastomers based on isosorbide. *Eur. Polym. J.* 83:161–172.
[9] Yang, Y., J., Huang, R. Zhang, and J. Zhu. 2017. Designing bio-based plasticizers: effect of alkyl chain length on plasticization properties of isosorbide diesters in PVC blends. *Mater. Des.* 126:29–36.
[10] Inayat, A., A. V. Assche, J. H. Clark, and T. J. Farmer. 2018. Greening the esterification between isosorbide and acetic acid. *Sust. Chem. Pharm.* 7:41–49.
[11] Hammami, N., M. Majdoub, and J. P. Habas. 2017. Structure-properties relationships in isosorbide-based polyacetals: influence of linear or cyclic architecture on polymer physicochemical properties. *Eur. Polym. J.* 93:795–804.
[12] Eo, Y. S., H. W. Rhee, and S. Shin. 2016. Catalyst screening for the melt polymerization of isosorbide-based polycarbonate. *J. Ind. Eng. Chem.* 37:42–46.
[13] Chatti, S., G. Schwarz, and H. R. Kricheldorf. 2006. Cyclic and noncyclic polycarbonates of isosorbide(1,4: 3,6-Dianhydro-D-glucitol). *Macromolecules* 39:9064–9070.
[14] Varkey, E. C., and K. Sreekumar. 2010. Isosorbide based chiral polyurethanes: optical and thermal studies. *J. Mater. Sci.* 45:1912–1920.
[15] Caouthar, A., P. Roger, M. Tessier, S. Chatti, J. C. Blais, and M. Bortolussi. 2007. Synthesis and characterization of new polyamides derived from di(4-cyanophenyl)isosorbide. *Eur. Polym. J.* 43:220–230.
[16] Fertier, L., M. Ibert, C. Buffe, R. S. Loup, C. Joly-Duhamel, J. J. Robin, and O. Giani. 2016. New biosourced UV curable coatings based on isosorbide. *Prog.Org. Coat.* 99:393–399.
[17] Casarano, R., R. Bentini, V. B. Bueno, T. Iacovella, F. B. F. Monteiro, F. A. S. Iha, A. Campa, D. F. S. Petri, M. Jaffe, and L. H. Catalani. 2009. Enhanced fibroblast adhesion and proliferation on electrospun fibers obtained from poly(isosorbide succinate-b-L-lactide) block copolymers. *Polymer* 50:6218–6227.
[18] Besse, V., R. Auvergne, S. Carlotti, G. Boutevin, B. Otazaghine, S. Caillol, J. P. Pascault, and B. Boutevin. 2013. Synthesis of isosorbide based polyurethanes: an isocyanate free method. *React. Funct. Polym.* 73: 588–594.
[19] Yabuki, A., W. Urushihara, J. Kinugasa, and K. Sugano. 2010. Self-healing properties of TiO_2 particle–polymer composite coatings for protection of aluminum alloys against corrosion in seawater. *Mater. Corros.* 61: 1–6.
[20] Li, W., H. Tian, and B. Hou. 2012. Corrosion performance of epoxy coatings modified by nanoparticulate SiO_2. *Mater. Corros.* 63:44–54.
[21] Fihri, A., D. Abdullatif, H. B. Saad, R. Mahfouz, H. Al-Baidary, and M. Bouhrara. 2019. Decorated fibrous silica epoxy coating exhibiting anti-corrosion properties. *Prog. Org. Coat.* 127:110–116.
[22] Yarahmadi, E., K. Didehban, M. G. Sari, M. R. Saeb, M. Shabanian, F. Aryanasa, P. Zarrintaj, S. M. R. Paran, M. Mozafari, M. Rallini, and D. Puglia. 2018. Development and curing potential of epoxy/starch-functionalized graphene oxide nanocomposite coatings. *Prog.Org. Coat.* 119:194–202.

[23] Sambyal, P., G. Ruhi, S. K. Dhawan, B. M. S. Bisht, and S. P. Gairola. 2018. Enhanced anticorrosive properties of tailored poly(aniline-anisidine)/chitosan/SiO_2 composite for protection of mild steel in aggressive marine conditions. *Prog. Org. Coat.* 119:203–213.

[24] Karami, Z., O. M. Jazani, A. H. Navarchian, and M. R. Saeb. 2018. State of cure in silicone/clay nanocomposite coatings: the puzzle and the solution. *Prog. Org. Coat.* 125:222–233.

[25] Alam, M., N. M. Alandis, and N. Ahmad. 2017. Development of poly(urethane-ester)amide from corn oil andtheir anticorrosive studies. *Int. J. Polym. Anal. Charact.* 22:281–293.

[26] Alam, M., and N. M. Alandis. 2012. Microwave-assisted preparation of urethane-modified polyetheramide coatings from Jatropha seed oil. *High Perform. Polym.* 24:538–545.

[27] Alam, M., F. Zafar, and E. Sharmin. 2013. *Advanced Functional Polymers and Composites: Materials, Devices and Allied Applications*. 1st ed., p. 128. USA: Nova Sci. Publishers, Inc.

[28] Khodabakhshi, J., H. Mahdavi, and F. Najafi. 2019. Investigation of viscoelastic and active corrosion protection properties of inhibitor modified silica nanoparticles/epoxy nanocomposite coatings on carbon steel. *Corros. Sci.* 147:128–140.

[29] Khajouei, A., E., Jamalizadeh, A. H. Jafari, and S. M. A. Hosseini. 2014. Layer-by-layer surfactants on silica nanoparticles for active corrosion protection. *Corros. Eng. Sci. Technol.* 49:743–748.

[30] Ramezanzadeh, B., S. Niroumandrad, A. Ahmadi, M. Mahdavian, and M. H. M. Moghadam. 2016. Enhancement of barrier and corrosion protection performance of anepoxy coating through wet transfer of amino functionalized grapheneoxide. *Corro. Sci.* 103:283–304.